INTERNATIONAL JOURNAL OF CLIMATOLOGY
Int. J. Climatol. **35**: 1342–1353 (2015)
Published online 9 June 2014 in Wiley Online Library
(wileyonlinelibrary.com) DOI: 10.1002/joc.4060

RMetS
Royal Meteorological Society

Dynamical seasonal predictability of the Arctic Oscillation using a CGCM

Jianqi Sun[a,b] and Joong-Bae Ahn[b*]

[a] *Nansen-Zhu International Research Centre (NZC), Institute of Atmospheric Physics, Chinese Academy of Sciences, Beijing, China*
[b] *Division of Earth Environmental System, Pusan National University, South Korea*

ABSTRACT: The potential dynamical predictability of the winter Arctic Oscillation (AO) is investigated using the ensemble hindcast from the Pusan National University coupled general circulation model (PNU-CGCM) over the 30-year period of 1981–2010. The analysis indicates that PNU-CGCM can not only reproduce the spatial distribution of the AO but also significantly simulate the AO's temporal variability. In addition, the coupled model performs well in terms of predicting the AO's impact on the Northern Hemisphere winter climate. These results reveal the coupled model's potential for dynamical forecasting of the climate over the mid-latitude to high latitude.

KEY WORDS Arctic Oscillation; CGCM; predictability; ensemble hindcast; winter climate

Received 18 July 2013; Revised 9 April 2014; Accepted 5 May 2014

1. Introduction

The Arctic Oscillation (AO) is the dominant mode of atmospheric circulation over the Northern Hemisphere (NH) (Thompson and Wallace, 1998). It primarily features a large-scale seesaw pattern between the Arctic Basin and the NH mid-latitudes, which reflects the surface signature of the modulations in the strength of the polar vortex.

Since the pioneering research of Thompson and Wallace (1998), the variability and impact of the AO have been extensively studied. The AO shows not only a strong interannual variability but also a remarkable decadal variability (Thompson *et al.*, 2000), which exerts a profound impact on the NH climate, producing anomalies in the NH air temperature and precipitation (e.g. Thompson and Wallace, 1998, 2000, 2001; Rigor *et al.*, 2000; Thompson *et al.*, 2000), sea ice and snow cover (e.g. Wang and Ikeda, 2000; Bamzai, 2003; Gong *et al.*, 2007), East Asian dust events (e.g. Kang and Wang, 2005; Gong *et al.*, 2006), and the Asian monsoon system (e.g. Gong *et al.*, 2001; Wu and Wang, 2002; Gong and Ho, 2003; Ju *et al.*, 2005). In addition, the AO can also influence the Siberian High, Aleutian low, and the Pacific Decadal Oscillation (Overland *et al.*, 1999; Gong *et al.*, 2001; Sun and Wang, 2006). Thus, exploring the AO predictability is important as it will allow us to improve the seasonal prediction of the NH climate to some extent.

In investigating the predictability of the AO, most previous studies have focused on short-term forecasts. For example, the Climate Prediction Center of the National Oceanic and Atmospheric Administration (NOAA) produces 1- to 2-week forecasts of the AO variability using the Global Forecast System model. Baldwin *et al.* (2003) found that the persistent circulation anomalies over the lowermost stratosphere have the potential for predicting the winter behaviour of the AO. Subsequent studies using numerical experiments have indicated that the variability of the stratosphere has potential prediction value for the tropospheric AO, but the prediction depends mainly on the stratosphere internal variability: The higher predictability of surface AO can be obtained only for the stratosphere sudden warming stage of the polar-night jet oscillation (Kuroda, 2008). For other stratosphere status, its prediction value for the tropospheric AO is weak.

Seasonal forecasting by numerical modelling is limited by the chaotic nature of the atmosphere. Generally, after about 2 weeks, the initial conditions of the atmosphere do not have much influence in shaping the future state of the atmosphere. Therefore, for seasonal forecasts, the most useful information comes from the low-varying and long-memory lower boundary (Derome *et al.*, 2005). In the current numerical seasonal forecast system, the variability of the sea surface temperature (SST), especially that of the tropical Pacific SST, is the major factor on which seasonal climate forecasting is based. Using an atmospheric general circulation model (AGCM) with the prescribed lower boundary, Derome *et al.* (2005) investigated the predictability of the dynamical method for the AO. They found that the AGCM shows a statistically significant ability to forecast the AO in the winter.

Unlike the AGCM with prescribed low-boundary conditions, low-boundary conditions in coupled models are subject to change through interactive processes with ocean and sea ice. The predictability of the AO is also

* Correspondence to: J.-B. Ahn, Division of Earth Environmental System, Pusan National University, Pusan 609735, South Korea. E-mail: jbahn@pusan.ac.kr

investigated based on the coupled model. Using several coupled ocean–atmosphere models in the frame of the Development of a European Multimodel Ensemble system for seasonal to inTERannual prediction (DEMETER) project and seasonal forecast system of the European Centre for Medium-Range Weather Forecasts (ECMWF), Muller *et al.* (2005) investigated the predictability of the North Atlantic Oscillation (NAO), the regional manifestation of the AO, which also has a strong impact on climate over the North Atlantic region and even Asia (e.g. Wallace and Gutzler, 1981; Barnston and Livezey, 1987; Hurrell, 1995; Chang *et al.*, 2001; Li *et al.*, 2003; Yang *et al.*, 2004; Yu and Zhou, 2004; Furevik and Nilsen, 2005; Sun *et al.*, 2008, 2009; Yuan and Sun, 2009). They found that, on a seasonal timescale, the coupled model has low prediction skill for the NAO. The low capability of the winter NAO forecasts was also reported by Deque (2004) based on the coupled Meteo-France. Qian *et al.* (2011) also analysed the DEMETER coupled models' data for the predictability of the AO. They found that all seven models simulated a realistic AO pattern compared to the observation, while the coupled models could not significantly predict the AO's temporal variability.

Sun and Ahn (2011) comprehensively diagnosed the Pusan National University coupled general circulation model (PNU-CGCM), a participant model of Asia-Pacific Economic Cooperation (APEC) Climate Center (APCC) multi-model ensemble (MME) long-range prediction system (http://www.apcc21.net/eng/html/hapcc030001.html). By comparing with other coupled models, they found that the PNU-CGCM showed better predictability for SST and hence more realistic SST conditions for the atmospheric component. This raises the question of whether the better description of the SST variability in the coupled model can therefore improve the predictability of the AO, the largest circulation mode over the NH middle-to-high latitudes. Furthermore, if the PNU-CGCM has significant ability to forecast the AO, can the coupled model produce the impact of the AO on the NH climate, which is revealed in the observations? If so, the uncertainty for the NH climate seasonal forecast will be reduced remarkably. The aim of this study was to answer the above two questions.

This article is divided into six sections. The data sets and climate model are introduced in Section 2. In Section 3, the ability of the PNU-CGCM to predict the AO behaviour is investigated. Further, the simulation ability for the impact of the AO on the NH climate is explored in Section 4. Sections 5 and 6 contain the discussion and conclusion, respectively.

2. Data, model, and initialization

2.1. Observed data

The atmospheric data set applied in this study is an updated reanalysis produced by the National Centers for Environmental Prediction-Department of Energy (NCEP R-2) (Kanamitsu *et al.,* 2002). This data set is gridded at a 2.5° latitude by 2.5° longitude resolution and covers the period from 1979 onwards. The variables analysed include wind, geopotential heights, sea level pressure (SLP), and air temperature. Also the Global Precipitation Climatology Projection version 2.2 (GPCP v2.2) precipitation and the NOAA Optimum Interpolation SST version 2 (Reynolds *et al.*, 2002) data are used for the analysis.

2.2. Model

The PNU-CGCM is a part of the APCC MME prediction system. PNU-CGCM v1.0 is a fully coupled ocean–atmosphere–land–sea-ice model (Sun and Ahn, 2011). The atmospheric component of the PNU-CGCM (Sun and Ahn, 2011) is the 18-vertical layer NCEP Community Climate Model version 3 (CCM3 T42) (Hurrell *et al.*, 1998) with a horizontal resolution of 2.8125°. The upper level of the AGCM is limited to 2.9 hPa. The oceanic component of the CGCM is the GFDL Modular Ocean Model version 3 (MOM3) (Pacanowski and Griffies, 1998), which has 40 vertical levels with the same horizontal resolution of 2.8125° as the AGCM in longitude. However, it has a variable grid in latitude with finer resolution at the equatorial region to resolve tropically trapped ocean waves, which seem to play an important role in the ENSO-related ocean dynamics, i.e. 0.7° at lower latitudes, below 30°; 1.4° at mid-latitude between 30° and 60°; and 2.8° at higher latitudes, above 60°. The sea-ice model used for the CGCM consists mainly of two parts: the Semtner-type thermodynamic part (Semtner, 1976) and the Los Alamos National Laboratory (LANL) Elastic-Viscous-Plastic (EVP) dynamic and transport part (Hunke and Dukowicz, 1997). The growth rate of the local sea ice and snow depth is calculated in the thermodynamic part, whereas the drifting velocity and transport of the sea ice are estimated in the dynamic and transport part. PNU-CGCM versions 1.0 and 1.1 are basically the same except that version 1.1 involves an ocean data assimilation process when producing the initial ocean conditions for the hindcast and prediction, whereas version 1.0 does not. In this study, the PNU-CGCM version 1.1 is used.

2.3. Initialization

To generate the atmospheric initial condition for the CGCM, we first produce the atmospheric mean states by running the AGCM for 10 years starting from an arbitrary atmospheric state (in this experiment, we used 15 September 1978 as the initial state) under given observed monthly mean SST (1978–2007) boundary conditions. The final state (15 September) of the atmosphere from the experiment is used as the initial condition of the 32-year, AMIP-type experiment, running from 15 September 1979 to 15 December 2010, inclusive. The model results from the AMIP-type reproduction experiment are, in turn, used as the atmospheric initial condition of the ensemble CGCM hindcasts. The initial conditions for the CGCM land surface variables obtained from the similar AMIP-type reproduction experiment with the same CCM3 AGCM are also used.

The monthly mean atmospheric conditions obtained from the AGCM spin-up experiment are also used as the upper boundary condition of the OGCM spin-up experiment. The OGCM is spun up for 100 years for the quasi-equilibrium ocean state by imposing monthly mean atmospheric boundary conditions repeatedly. Although 100 years of integration is not enough for the model to acquire a fully spun-up ocean state, we assume that the upper part of the ocean has reached an adequate quasi-equilibrium state, as our interest is mainly focused on the analysis and prediction of climates with a timescale of less than a year. As a next step, the reproduced atmospheric states for the period of 1979–2010 are used as the boundary condition of OGCM for the reproduction of the ocean states for the same period. Unlike the PNU-CGCM version 1.0 hindcast experiment, which uses the reproduced ocean states as the initial condition of the oceanic part of CGCM, the reproduced ocean states in the version 1.1 hindcast experiment are used as the background field for the ocean data assimilation. Here, the variational method using filter (VAF) method (Huang, 2000, Ahn *et al.*, 2005) is applied to the raw model data to assimilate the observed ocean temperature and salinity for the generation of the initial coupled ocean conditions. In particular, not only the Array for Real-time Geostrophic Oceanography (ARGO), Tropical Atmosphere and Ocean (TAO), and Expendable Bathythermographs (XBTs) *in situ* ocean observation data are used, but also the Global Ocean Data Assimilation System (GODAS) data are utilized in the ocean data assimilation to improve the initial ocean fields. The reason for using GODAS, which is already 3D assimilated ocean data, is to give the model more secure dynamical and thermodynamical balances. Otherwise, it would be difficult for us to achieve the balances due to the sparse and irregular distribution of ocean observations.

The atmospheric and land surface initial conditions obtained from the AGCM reproduction experiments, together with the oceanic initial condition from the OGCM reproduction and data assimilation, are all used as the initial conditions of the version 1.1 hindcast experiments. The main purpose of this rather sophisticated procedure in generating the initial conditions of the CGCM is to give sufficient memory to the coupled model, so as to minimize the initial shock and/or drift that might occur during the adjustment period of the initial coupling.

The PNU-CGCM hindcasts for January–February–March (JFM), recognized as the AO active season (Thompson and Wallace, 2000), over the 30-year period of 1981–2010, with initial conditions from October and December corresponding to 2.5- and 0.5-month lead hindcasts, respectively, are used to investigate the dynamical predictability of the AO. The ensemble method in this study is a time-lagged method (Brankovic *et al.*, 1990; Trilaksono *et al.*, 2012). The initial conditions for each CGCM hindcast are taken from five different days (the 12th, 13th, 14th, 15th, and 16th day) of October and December, approximately 2.5 and 0.5 months, respectively, prior to the beginning of January, for the JFM ensemble hindcasts. Each ensemble member consists of 30 individual runs. Thus, we have a 30-year averaged model monthly climatology for each lead month and the individual 3-month hindcast has five ensemble members. The monthly mean state of the CGCM hindcast is defined as the norm of the five ensemble means of the 30-year average for each lead of the individual runs. Thus, each lead and run has its own mean model climate, and the anomaly is defined as the deviation from the mean of the corresponding lead and run.

After analysis, we found that the coupled model can predict the AO spatial pattern in both hindcasts, but the model can only significantly predict the temporal variability of the AO at the 0.5- to 2.5-month lead hindcast. Thus, the following analysis shows the result from the 0.5- to 2.5-month lead hindcasts.

3. The predictability of the PNU-CGCM for the AO pattern

Generally, the AO mode is identified as the leading empirical orthogonal function (EOF) for atmospheric circulations over the NH (northward of 20°N). Hence, the EOF analysis is first applied to the observation and PNU-CGCM hindcasts for the 30-year period of 1981–2010.

Figure 1(a) shows the first leading pattern of the SLP over the NH (north of 20°N) from the observations. The structure of the NH SLP anomalies is virtually identical to that derived from previous analysis (e.g. Thompson and Wallace, 1998). With a positive-phase AO pattern, a negative anomalous centre lies over the North Polar region and two positive anomalous centres lie over the North Pacific and North Atlantic–western Europe regions. Comparing Figure 1(b) with 1(a), we find that the model presents a quite realistic AO pattern, with a pattern correlation of 0.74 with the observation. The model AO explains 52.7% of the variability, somewhat higher than the observation with a value of 34.3%. The spatial structure of the leading mode of the 850-hPa geopotential height is highly consistent with that of the SLP field in both the observations and the model. The explained variances are also similar over these two levels.

Over the lower levels, the AO pattern shows a zonally asymmetric structure with two positive centres over the North Pacific and Atlantic, which is mainly induced by the land–sea distribution. Meanwhile, over the middle and upper levels, the influence of the land–sea distribution becomes weaker, and consequently the leading EOF mode is more zonally symmetric than at the lower levels. As seen in Figure 1(e), the positive anomalies over the middle latitudes become an almost closed ring in the observations, surrounding the north polar negative value region. The coupled model did not capture this change in the AO pattern; the positive values still show two centres over the NH middle latitudes. However, the coupled model simulated pattern is generally similar to the observations over the middle and upper levels. The pattern correlations are 0.73 and 0.71 over 500 and 200 hPa, respectively.

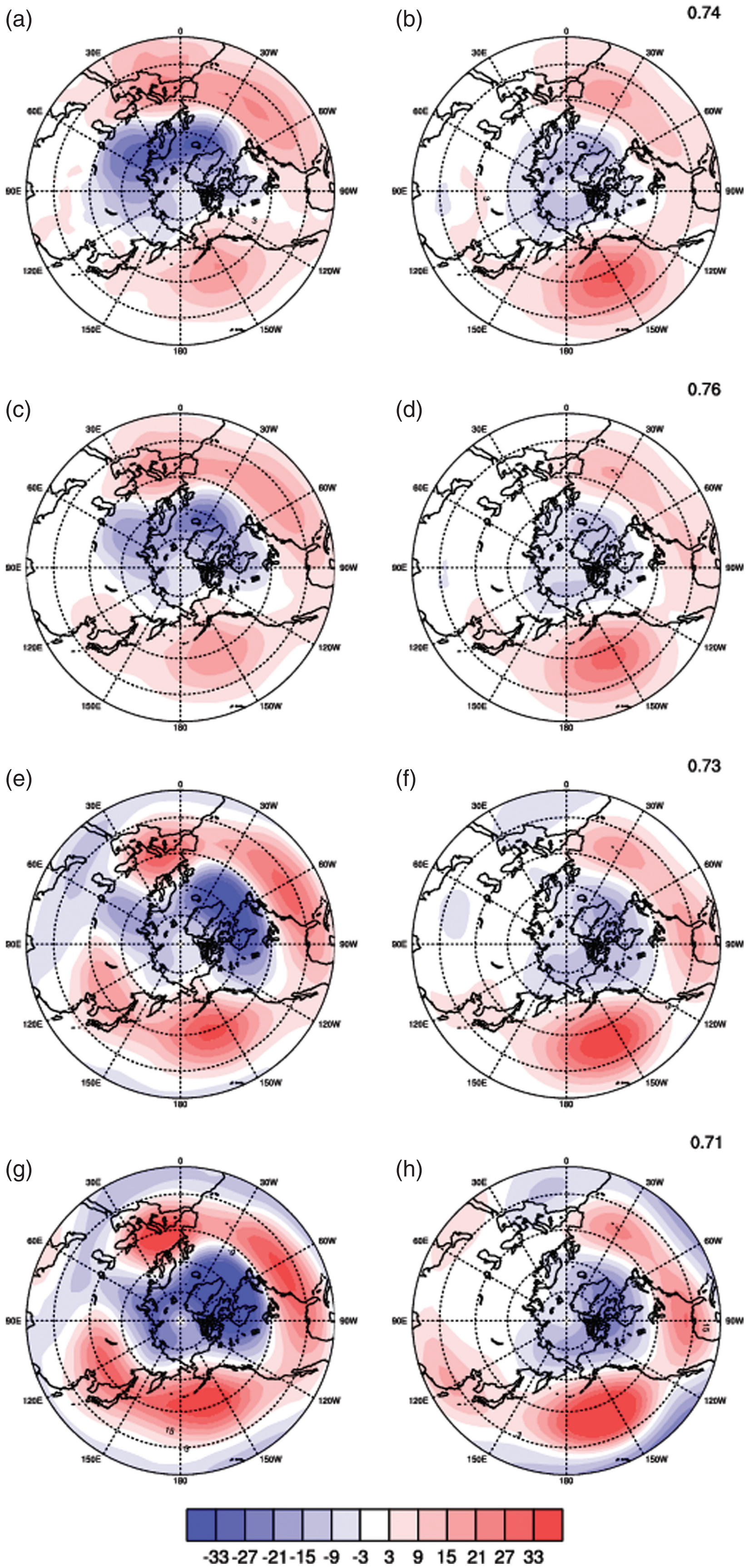

Figure 1. Spatial distributions of the leading EOF modes over 1981–2010. The values at the top right of each figure are the spatial correlation coefficients between the observation and simulation at each level.

The AO indices over difference level are presented in Figure 2. The observed AO indices are defined as the time components of the first leading EOF modes over different levels. To keep the exactly same pattern of AO for the observations and the model, it is more reasonable to project the simulated anomaly onto the observed leading EOF modes to obtain the model AO index. The figure suggests that the coupled model also has the ability to predict the temporal variability of the AO. In particular, on the surface level, the two time series show a highly consistent variability, with a correlation coefficient of 0.60, which is significant at the 99% confidence level. This means that the coupled model can predict about 36% of the AO variability. At higher atmospheric level, the correlation of the time series between the observed and predicted data is reduced. Over the 200-hPa level, the correlation is 0.43, which is also significant at the 95% confidence level. This result indicates that the predictability of the AO variability is more significant over the lower level. The above analysis suggests that the PNU-CGCM has a good ability to predict both the spatial pattern and the temporal variability of the AO.

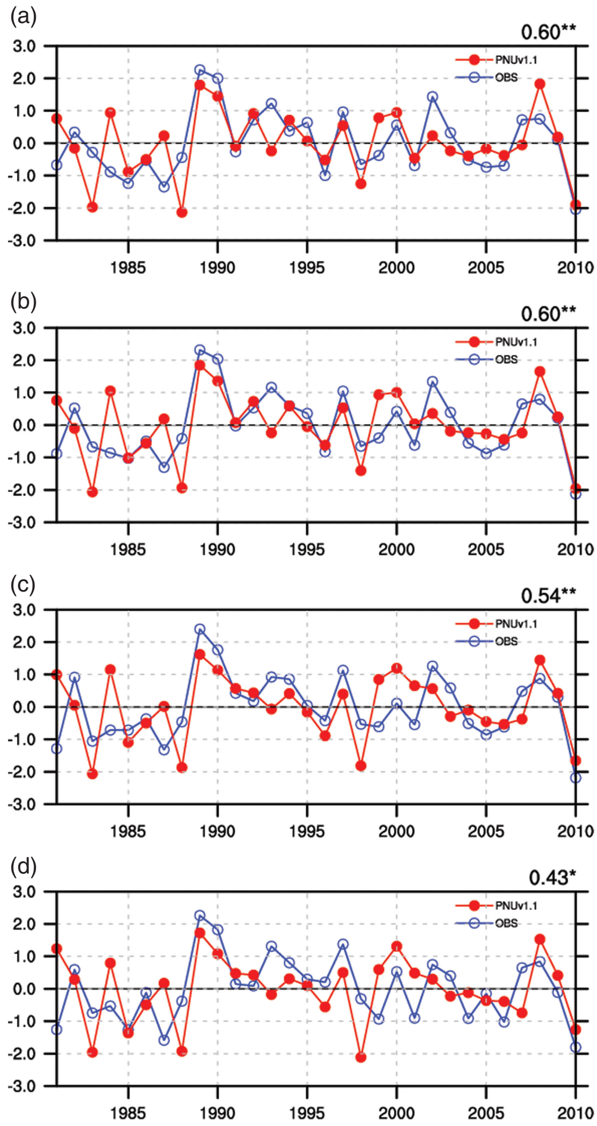

Figure 2. Normalized time series of the AO indices at different levels over 1981–2010. The observed AO indices are defined as the time components of the first leading EOF modes. The model AO indices are obtained by projecting the simulated anomaly onto the observed leading EOF modes. The values at the top right of each row are the temporal correlation coefficients between the observation and simulation at each level. * and ** indicate the 98% and 99% levels of confidence, respectively.

4. The ability of the PNU-CGCM to predict the AO's impact on the NH climate

As reviewed in Section 1, the AO has a profound impact on the NH climate. In Section 3, we indicated that the PNU-CGCM has the ability to predict the AO. If the PNU-CGCM can also predict the AO's impact on the NH climate, it will reduce the uncertainty in the predictions for the NH winter climate. Thus, the AO-related climate in both the observation and the coupled model are compared in this section.

Figure 3(a) shows the winter mean 850-hPa winds and surface air temperature (SAT) regressed upon the AO index. The observed AO index is referred to as the normalized time component of the first leading EOF mode of the SLP, similar to a previous study (Thompson and Wallace, 1998). The model AO index is obtained by projecting the simulated SLP anomaly onto the observed leading EOF mode of SLP. By this way, we have exactly the same AO pattern for the observation and the model. Figure 3 shows that the distribution of the AO-related winds and air temperature is reminiscent of that in the study of Thompson and Wallace (1998). Corresponding to a positive AO pattern, there are positive SAT anomalies over the northern part of the Eurasian Continent and eastern United States, and negative anomalies over the southern part of the Eurasian Continent and eastern Canada–Greenland region. This distribution of the SAT anomalies is attributed to the temperature advection caused by the AO-related winds. For example, the positive-phase AO is associated with an anomalous westerly over northern Europe, which brings relative warm air from the North Atlantic, with an anomalous southwesterly flow over western North Asia, which brings relatively warm air from the mid-latitude Asian region, and with an anomalous easterly and southeasterly flow over northern East Asia, which brings relatively warm air from the western North Pacific and mid-East Asia regions. In contrast, over the southern part of the Eurasian Continent, as the anomalous northerly flow associated with the positive-phase AO brings cold air from higher latitudes, the air temperature over this region will be cold. The cold region over eastern Canada–Greenland is a result of the strong anomalous northeasterly cold air advection from the North Polar region, and the warm region over eastern United States is affected by the anomalous easterly flow with warm air advection from the North Atlantic. These features of the AO-related observed SAT and winds are all well captured by PNU-CGCM, as shown in Figure 3(b), although the significant areas have

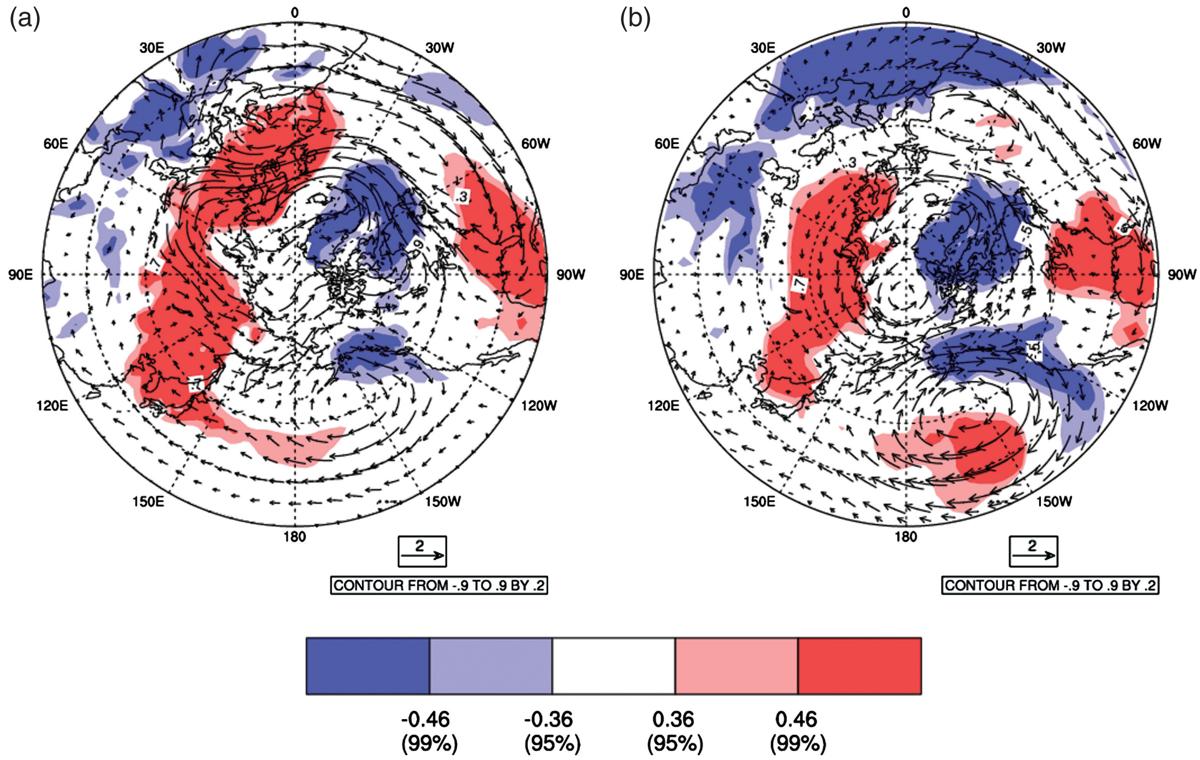

Figure 3. Regression patterns of the 850-hPa horizontal winds and correlation patterns of the SAT with the AO index derived from SLP over 1981–2010. The shading areas indicate the 95% and 99% levels of confidence.

shrunk somewhat over the north Eurasian Continent and expanded over the North Pacific.

Precipitation is another important climate variable that is used to evaluate the model's simulation. Generally, precipitation is one of the most difficult variables to predict with numerical models. Here, the forecasting skill of the PNU-CGCM on the AO-related precipitation is further checked. As shown in Figure 4, compared to the winds and temperature, the coupled model exhibits very limited ability to reproduce the observed precipitation responses. For example, the strongest correlations in the model always located over the oceans. The model produces a more significant precipitation signal over the middle and northern Asian Continent, and it shows a wrong prediction over eastern North America compared to the observation.

On the other hand, however, we find that the PNU-CGCM shows some predictive ability for the AO-related strong NH winter precipitation signals. Over Europe, the AO-related precipitation anomalies show the main large-scale feature with dipole anomaly between the Northern Europe and Mediterranean region. The PNU-CGCM did not well simulate the spatial scale of this dipole pattern. But it produces the anomalous precipitation signal. In a positive-phase AO year, the western wind from the mid-North Atlantic to northern Europe is strengthened, bringing more moisture to northern Europe, and consequently more rainfall there. In contrast, over southern Europe, the westerly wind from the North Atlantic is weakened in a positive-phase AO year, resulting in less precipitation over the region. Over eastern China, because of the AO-related easterly wind from the North Pacific, more moisture will be transported to this region, thereby enhancing the precipitation. These three AO-related strong precipitation anomalies are well predicted by the PNU-CGCM, although the extent and position of the significant areas have some visible differences between the observation and model simulation.

To further illustrate the ability of the PNU-CGCM to predict the AO impact, we calculated the difference forecast skill of SAT and precipitation between with and without the impact of the AO. The forecast skill is reflected by the temporal correlation coefficients between the observation and model simulation, and the AO's impact is removed by the linear regression method. From Figure 5(c), we can find that the predictability of the PNU-CGCM has an increase for SAT when the AO signal is included, in particular over the land regions where the AO has strong impact on the observation (Figure 3(a)). Figure 5(b) shows the precipitation situation. When compared with the temperature, the PNU-CGCM predictability for the precipitation is lower. However, if the AO's impact is included, we can find that the CGCM predictability for the Northern Europe and Mediterranean region, the AO major impact region, has improved (Figure 5(b)). These results indicate that the CGCM can improve the prediction of winter climate if it has good predictability for the AO.

Over the NH winter, an important active climate system is the East Asian winter monsoon (EAWM). Some previous studies revealed that the AO has a remarkable impact on the EAWM (Gong *et al.*, 2001; Wu and Wang,

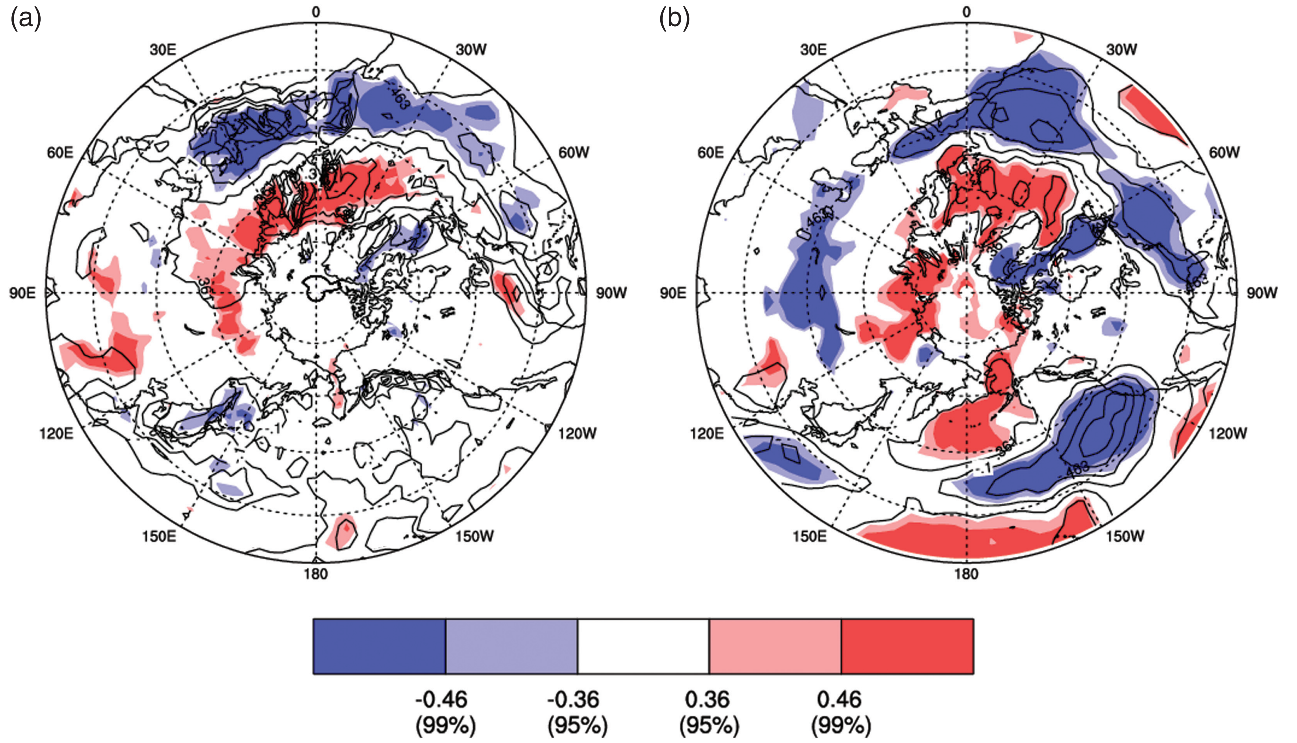

Figure 4. Correlation patterns of the precipitation with the AO index derived from SLP over 1981–2010. The shading areas indicate the 95% and 99% levels of confidence.

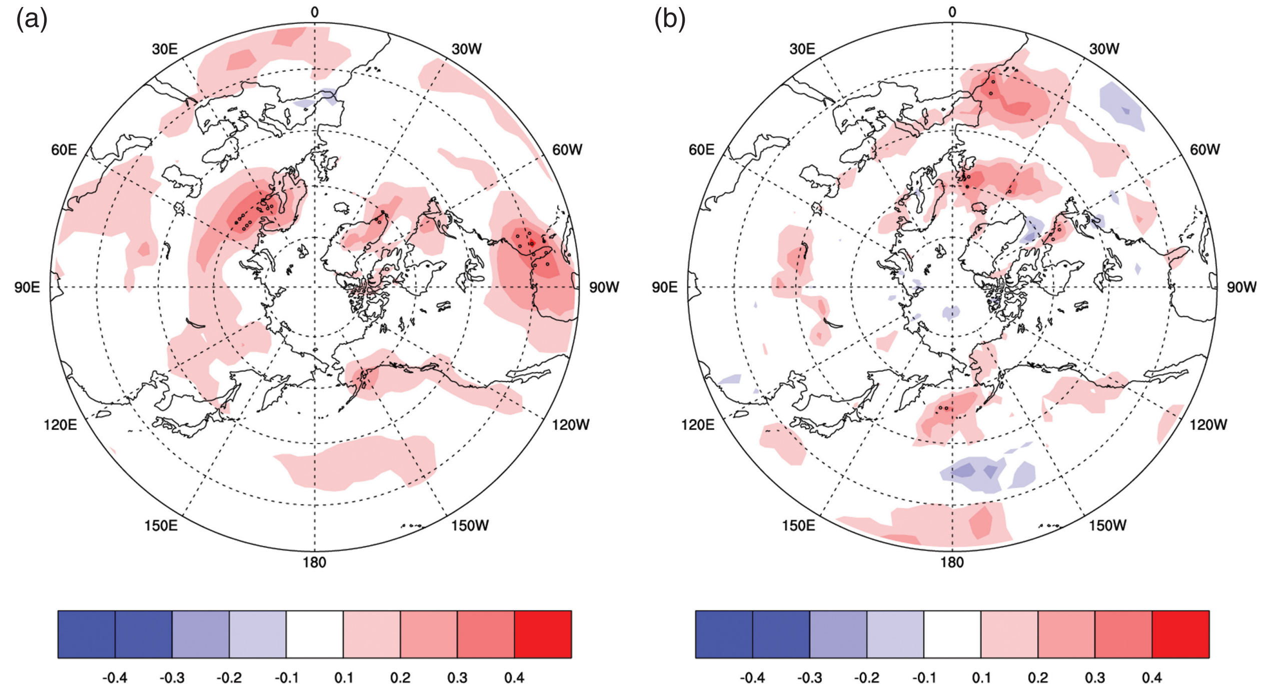

Figure 5. Difference maps of the temporal correlation coefficients between the observation and simulation for (a) SAT and (b) precipitation between with and without AO impact. The dotted areas indicate where the difference between two correlation coefficients is above 90% level of confidence.

2002). From the pronounced AO-related wind analysis, qualitatively speaking, the PNU-CGCM can predict the impact of the AO on the EAWM. Moreover, we use several EAWM indices to investigate the model's predictability quantitatively. Here, three EAWM indices are used, which are defined as (1) the averaged mean of the 850-hPa wind velocity over the region (25–50°N, 115–145°E) ($\mathrm{EAWMI}_{\text{Wang and Jiang}}$) (Wang and Jiang, 2004); (2) the averaged mean of the 500-hPa geopotential height over the region (30–45°N, 125–145°E) ($\mathrm{WAWMI}_{\text{Sun and Li}}$) (Sun and Li, 1997); and (3) the difference in the 300-hPa zonal wind between region (27.5–37.5°N, 110–170°E)

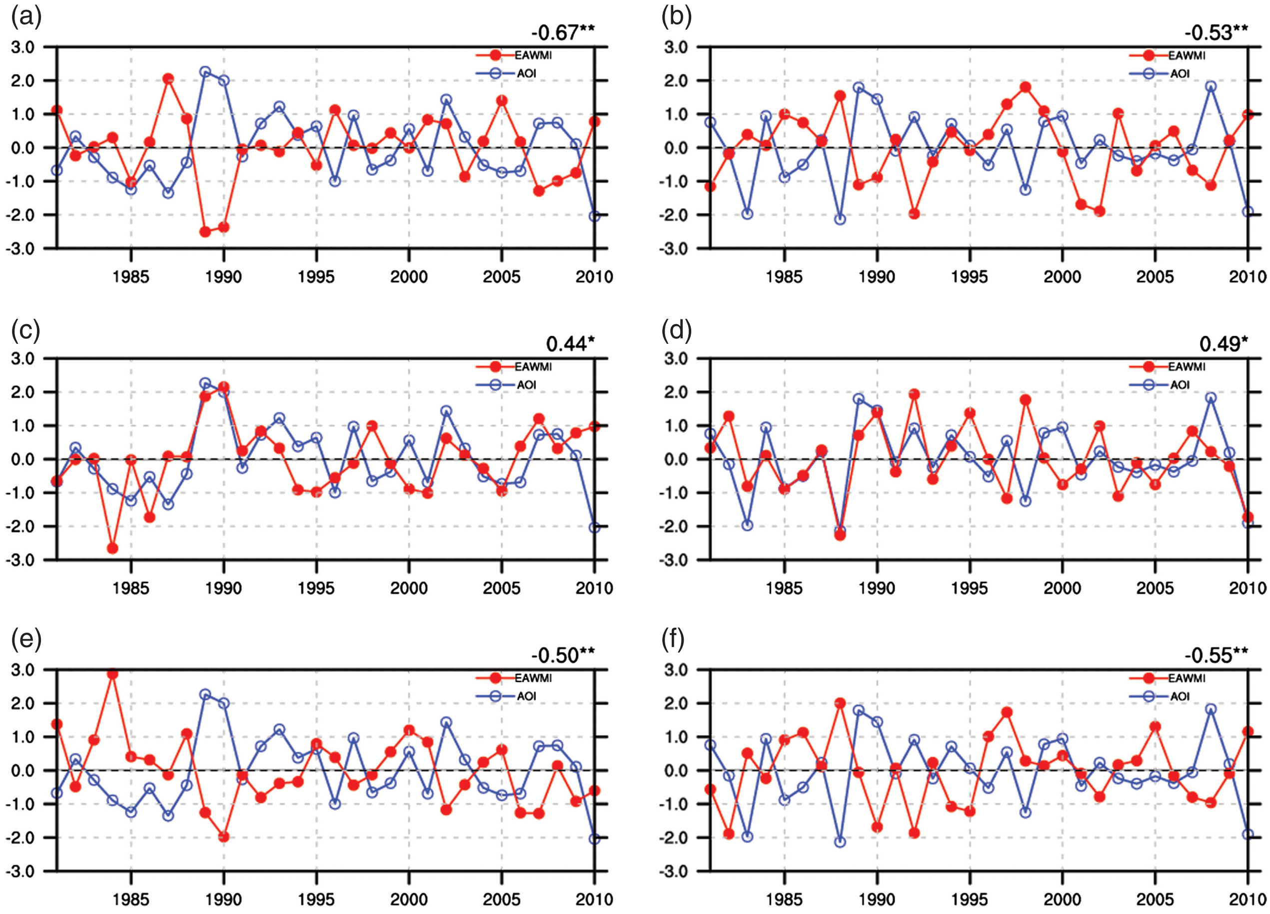

Figure 6. Time series of the AO index derived from SLP and three EAWM indices in the observation and simulation over 1981–2010. * and ** indicate the 98% and 99.9% levels of confidence, respectively.

and region (50–60°N, 80–140°E) ($\mathrm{EAWM_{Jhun\ and\ Lee}}$) (Jhun and Lee, 2004). Figure 6 shows the AO index and three EAWM indices in the observation and simulation. It suggests that, similar to the observation, the AO and EAWM indices in the simulation are also consistent with each other. The correlations between the predicted AO and WAWM indices are −0.53, 0.49, and −0.55, which are all significant at the 95% confidence level. Thus, the PNU-CGCM has good predictive ability for the EAWM. The observed correlations of AO and these three EAWM indices are −0.67 for $\mathrm{EAWMI_{Wang\ and\ Jiang}}$, 0.44 for $\mathrm{EAWMI_{Sun\ and\ Li}}$, and −0.50 for $\mathrm{EAWMI_{Jhun\ and\ Lee}}$, which are all significant at the 95% confidence level.

The above analysis implies that the PNU-CGCM can not only predict the AO spatial–temporal variability but can also predict its impact on the NH winter climate. The model thus has a promising potential to reduce the predicting uncertainty for the NH climate.

5. Discussion

The dynamical diagnosis of the observations and model simulation indicates that atmospheric internal processes involving eddy-mean-flow interactions play an important role in generating the AO (Limpasuvan and Hartmann, 1999, 2000). Because of the chaotic nature of the atmosphere, the atmosphere on its own lacks the mechanisms to generate predictable variations on seasonal timescales. Therefore, the persistence and predictability of the AO could result from the influence of the low-varying boundary conditions, especially the SST.

Figure 7(a) shows the middle-level AO index-related SST anomalies. It suggests that significant signals dominate the North Pacific and Atlantic. Over the North Pacific, positive anomalies are observed over the western to middle Pacific, surrounded by negative anomalies. Over the North Atlantic, the SST anomalies show a tripole pattern with a positive area in the centre and negative areas on both sides. In general, it is considered that the mid-latitude SST variability is forced predominantly by the atmosphere (e.g. Frankignoul *et al.*, 1998), while some recent studies revealed that the mid-latitude SST can also generate feedback to the atmosphere, which can sustain the atmospheric pattern. Peng *et al.* (2003) studied the atmospheric response to the North Atlantic SST tripole pattern, which is similar to the AO-related SST anomalies over the North Atlantic (Figure 7(a) and (c)). They obtained an NAO-like dipole with an equivalent barotropic structure over the Atlantic. Liu and Wu (2004) investigated the atmospheric response to a mid-latitude winter SST anomaly over the western to central North Pacific, similar to the position

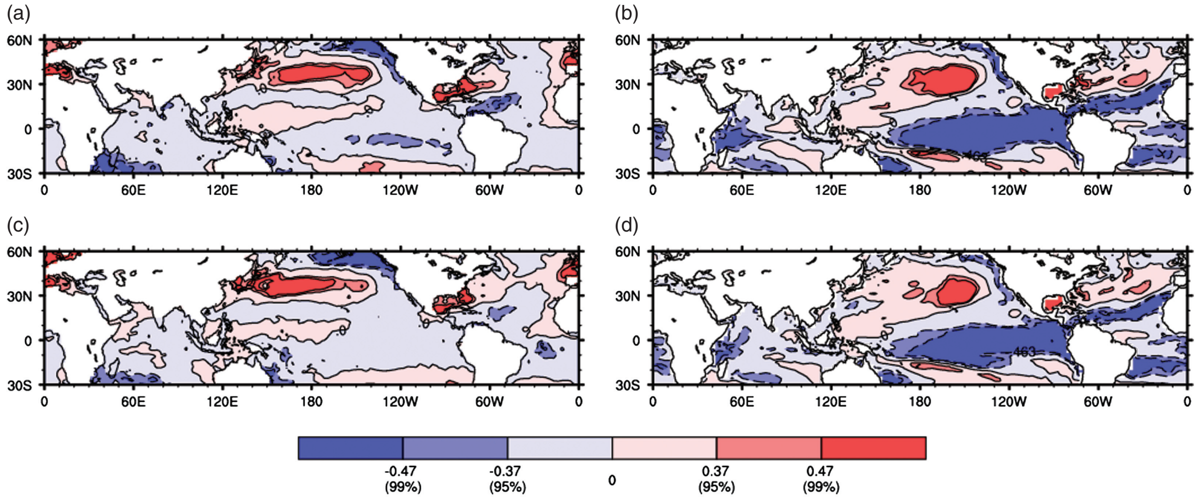

Figure 7. Correlation maps of the SST and the AO indices in the observation and simulation over 1981–2010. The shading areas indicate the 95% and 99% levels of confidence.

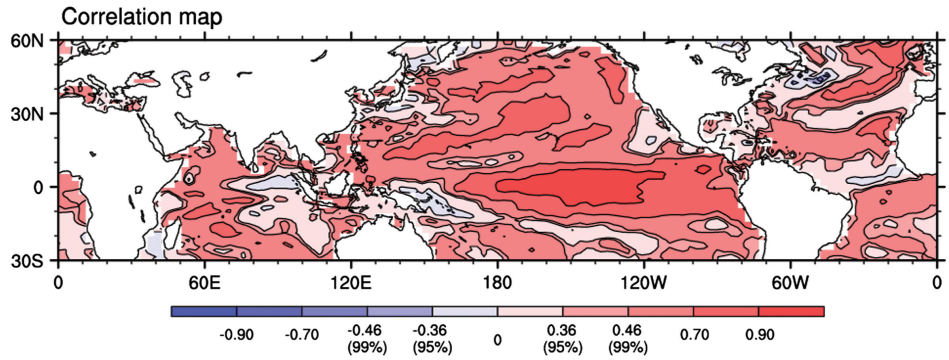

Figure 8. Map of the SST correlation between the observation and simulation over 1981–2010.

of the AO-related positive SST anomalies over the North Pacific. They found that the response of the atmosphere shows an AO-like pattern over the NH. They also revealed that a full coupling between the atmosphere and ocean can produce the strongest response.

Besides the NH extratropics, the middle-level AO index-related SST anomalies show that there are also significant SST signals over the middle and eastern tropical Pacific (Figure 7(a)). The tropical link of the AO is in agreement with previous studies (Lin *et al.*, 2002; Greatbatch *et al.*, 2003; Lin *et al.*, 2005; Tang *et al.*, 2007). Using an atmospheric model, Lin *et al.* (2002) and Greatbatch *et al.* (2003) revealed that tropical thermal forcing plays an important role in the AO variability. Further, Lin *et al.* (2005) developed a correction scheme for seasonal predictions using the tropical Pacific SST signal. They found that this scheme can significantly increase the predictive capability of two GCMs in the seasonal predictions of the AO. Based on information theory, Tang *et al.* (2007) also pointed out that a reliable prediction for the AO is usually linked to strong SST forcing in the tropical central Pacific and the mid-western North Pacific, whereas a poor prediction is associated with weak SST forcing in the two regions. Hence, the interaction between the AO and its related SST could sustain the AO pattern and improve its predictability on a seasonal timescale.

Figure 7(b) and (d) presents the corresponding situations in the coupled model. The correlation maps suggest that the AO-related anomalous SST patterns in the simulations have some differences with the observation. For example, the positive centre over North Pacific shifts more eastward. The SST signal over the North Atlantic and tropical Pacific is much stronger than in the observation. However, for the general features, the PNU-CGCM still produces the observed SST anomalous distribution, which indicates that the PNU-CGCM can provide a good description of the observed relationships between the AO and the SST.

In addition, the PNU-CGCM also shows a strong ability to reproduce the observed SST variability. As shown in Figure 8, the correlation coefficients between the simulated and observed SSTs are significant at the 99% confidence level over most parts of the ocean, especially over the tropical and NH oceans, which means that the PNU-CGCM can provide a realistic boundary condition for the atmospheric model.

The above analysis demonstrates the good predictive ability of the PNU-CGCM for the SST variability. This in turn might have contributed to the significant prediction of

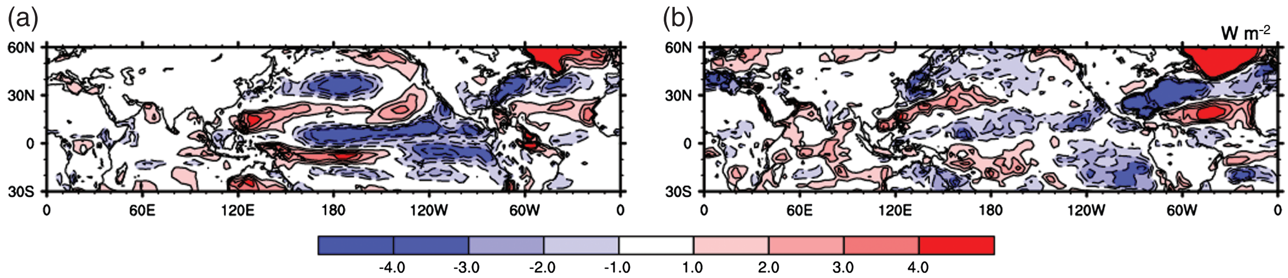

Figure 9. Regression patterns of turbulent heat flux (W m^{-2}) on AO index derived from SLP for the (a) reanalysis and (b) model.

the variability of AO. By means of a simple linear model, Bretherton and Battisti (2000) showed that when employing SST anomaly pattern produced by internal atmospheric dynamics as boundary conditions for an atmosphere model, one will always get a correlation between the forcing and atmosphere response. They consequently argued that it should be caution to using the mid-latitude SST to interpret the variability of the coupled system. Thus, the contribution of the good predictive ability of the SST to the high predictability of the AO still has uncertainty.

To further explore the possible mechanism for the AO prediction, we calculated the AO-related turbulent heat flux from both the reanalysis and PNU-CGCM. The turbulent heat is good variable to depict the air–sea interactions. As shown in Figure 9, we can find that, compared to the SST pattern, the AO-related heat fluxes show more similar pattern between the reanalysis and model, albeit there are still visible differences on magnitude and distribution. The air–sea interactions over the Northern Oceans and Tropical Pacific are the key regions for the variability of the AO, which is consistent with previous studies (Lin *et al.*, 2002; Greatbatch *et al.*, 2003; Peng *et al.*, 2003; Liu and Wu, 2004; Lin *et al.*, 2005; Tang *et al.*, 2007). These results indicate that the PNU-CGCM can well produce the AO-related air–sea interaction processes, and consequently significantly simulate the AO variability.

6. Conclusion

As a dominant pattern over the NH extratropics, the AO phenomenon is a major player in the NH climate. Thus, it is important to evaluate its predictability. In this study, based on the 30-year hindcast data of the PNU-CGCM, we investigated the predictability of AO as well as its impact on the NH climate. The results suggest that this coupled model has the capability to predict the AO spatial and temporal variability at 0.5- to 2.5-month lead. Furthermore, the observed relationships between the AO and NH air temperature, precipitation, and circulations are all well reproduced by the coupled model. These results indicate that the coupled model may also have the potential to predict the extratropical climate.

The correlation coefficients between AO indices and each member of five different integration-start days (the 12th, 13th, 14th, 15th, and 16th day) of December for SLP were 0.43, 0.43, 0.21, 0.34, and 0.43, respectively. This implies that 1-day lagged initial condition is sufficient to separate each ensemble as for the AO prediction concerns. Considering that the correlation coefficient of the simple composited ensemble with the index was 0.60, the ensemble hindcast also improved the predictability of AO remarkably. This implies that an individual member run always has less skill than the ensemble mean in the prediction of AO.

Generally, the coupled model shows better forecasting ability in the tropics than in the extratropics. As reviewed in Section 1, some models cannot depict the temporal variability of the AO, although they can simulate the spatial pattern of the AO. In contrast, our study indicates that the PNU-CGCM shows a significant predictability for both the AO spatial pattern and temporal variability, although the uppermost level of the atmospheric model is limited to 2.9 hPa. Although the importance of upper-level solar activity on AO has been suggested by many studies (e.g. Kodera, 2003; Kryjov and Park, 2007; Ahn and Kim, 2014), the reason for the improved AO predictability might be related with the initialization processes in generating the initial conditions of coupled ocean and land surface. Derome *et al.* (2005) also suggested that the most useful information for seasonal forecasts comes from the low-varying and long-memory lower boundary. The present study analysis has demonstrated the good simulation performance of the PNU-CGCM in oceanic conditions, in both the tropics and extratropics, and also in the air–sea interaction process associated with the AO, as shown in Figures 7–9, which might be an important reason for its high predictability for the AO. However, the possible reasons for the improvement need to be further investigated by intermodel comparison in the future.

Acknowledgements

This research was jointly supported by 'the Korea Meteorological Administration Research and Development Program under Grant CATER 2012-3083', 'the Special Fund for Public Welfare Industry (Meteorology) (GYHY201306026) of China', and 'the Jiangsu Collaborative Innovation Center for Climate Change'. The authors are grateful to Mr Lee, J. L. for his assistance in drawing figures of this manuscript.

References

Ahn JB, Kim HJ. 2014. Improvement of 1-month lead predictability of the wintertime AO using a realistically varying solar constant for a CGCM. *Meteorol. Appl.* **21**: 415–418, DOI: 10.1002/met.1372.

Ahn JB, Yoon YH, Cho EH, Oh H. 2005. A study of global ocean data assimilation using VAF. *J. Korean Soc. Oceanogr.* **10**: 69–78 (in Korean).

Baldwin MP, Stephenson DB, Thompson DWJ, Dunkerton TJ, Charlton AJ, O'Neill A. 2003. Stratospheric memory and skill of extended-range weather forecasts. *Science* **301**: 636–640.

Bamzai AB. 2003. Relationship between snow cover variability and Arctic Oscillation index on a hierarchy of time scales. *Int. J. Climatol.* **23**: 131–142.

Barnston AG, Livezey RE. 1987. Classification, seasonality and persistence of low-frequency atmospheric circulation patterns. *Mon. Weather Rev.* **115**: 1083–1126.

Brankovic C, Palmer TN, Molteni F, Tibaldi S, Cubasch U. 1990. Extended-range predictions with ECMWF models: time lagged ensemble forecasting. *Q. J. R. Meteorol. Soc.* **116**: 867–912.

Bretherton CS, Battisti DS. 2000. An interpretation of the results from atmospheric general circulation models forced by the time history of the observed sea surface temperature distribution. *Geophys. Res. Lett.* **27**: 767–770.

Chang CP, Harr P, Ju J. 2001. Possible roles of Atlantic circulations on the weakening Indian monsoon rainfall-ENSO relationship. *J. Clim.* **14**: 2376–2380.

Deque M. 2004. Seasonal prediction over the Atlantic by the French Weather Service. In *CLIVAR Publication* Series No. 81. Reading, UK, 10–16.

Derome J, Lin H, Brunet G. 2005. Seasonal forecasting with a simple general circulation model: predictive skill in the AO and PNA. *J. Clim.* **15**: 597–609.

Frankignoul C, Czaja A, L'Heveder B. 1998. Air–sea feedback in the North Atlantic and surface boundary conditions for ocean models. *J. Clim.* **11**: 2310–2324.

Furevik T, Nilsen JEO. 2005. Large-scale atmospheric circulation variability and its impacts on the Nordic Seas Ocean climate – a review. In *The Nordic Seas: An Integrated Perspective*. AGU Monograph **158**, Drange H , Dokken T, Furevik T, Gerdes R, Berger W (eds). AGU: Washington, DC, 105–136.

Gong DY, Ho C-H. 2003. Arctic oscillation signals in the East Asian summer monsoon. *J. Geophys. Res.* **108**(D2): 4066, DOI: 10.1029/2002JD002193.

Gong DY, Wang SW, Zhu JH. 2001. East Asian winter monsoon and Arctic Oscillation. *Geophys. Res. Lett.* **28**(10): 2073–2076.

Gong DY, Mao R, Fan YD. 2006. East Asian dust storm and weather disturbance: possible links to the Arctic Oscillation. *Int. J. Climatol.* **26**: 1379–1396.

Gong DY, Kim SJ, Chang HH. 2007. Arctic Oscillation and ice severity in the Bohai Sea, East Asia. *Int. J. Climatol.* **27**: 1287–1302.

Greatbatch RJ, Lin H, Lu J, Peterson KA, Derome J. 2003. Tropical/extratropical forcing of the AO/NAO, 2003: a corrigendum. *Geophys. Res. Lett.* **30**: 1738, DOI: 10.1029/2003GL017406.

Huang X-Y. 2000. Variational analysis using spatial filters. *Mon. Weather Rev.* **128**: 2588–2600.

Hunke EC, Dukowicz JK. 1997. An elastic–viscous–plastic model for sea ice dynamics. *J. Phys. Oceanogr.* **27**: 1849–1867.

Hurrell JW. 1995. Decadal trends in the North Atlantic Oscillation: regional temperatures and precipitation. *Science* **269**: 676–679.

Hurrell JW, Hack JJ, Boville BA, Williamson DL, Kiehl JT. 1998. The dynamical simulation of the NCAR Community Climate Model Version 3 (CCM3). *J. Clim.* **11**: 1207–1236.

Jhun JG, Lee EJ. 2004. A new East Asian winter monsoon index and associated characteristics of the winter monsoon. *J. Clim.* **17**(4): 711–726.

Ju JH, Lv JM, Cao J, Ren JZ. 2005. Possible impacts of the arctic oscillation on the interdecadal variation of summer monsoon rainfall in East Asia. *Adv. Atmos. Sci.* **22**: 39–48.

Kanamitsu M, Ebisuzaki W, Woollen J, Yang SK, Hnilo JJ, Fiorino M, Potter GL. 2002. NCEP-DEO AMIP-II Reanalysis (R-2). *Bull. Am. Meteorol. Soc.* **83**: 1631–1643.

Kang DJ, Wang HJ. 2005. Analysis on the decadal scale variation of the dust storm in North China. *Sci. China Ser. D Earth Sci.* **48**(12): 2260–2266.

Kodera K. 2003. Solar influence on the spatial structure of the NAO during the winter 1900–1999. *Geophys. Res. Lett.* **30**: 1175, DOI: 10.1029/2002GL016584.

Kryjov VN, Park C-K. 2007. Solar modulation of the El Nino/Southern Oscillation impact on the Northern Hemisphere annular mode. *Geophys. Res. Lett.* **34**: L10701, DOI: 10.1029/2006GL028015.

Kuroda Y. 2008. Role of the stratosphere on the predictability of medium range weather forecast: a case study of winter 2003–2004. *Geophys. Res. Lett.* **35**: L19701, DOI: 10.1029/2008GL034902.

Li SL, Robinson WA, Peng S. 2003. Influence of the North Atlantic SST tripole on northwest African rainfall. *J. Geophys. Res.* **108**(D19): 4594, DOI: 10.1029/2002JD003130.

Limpasuvan V, Hartmann DL. 1999. Eddies and the annular modes of climate variability. *Geophys. Res. Lett.* **26**: 3133–3136.

Limpasuvan V, Hartmann DL. 2000. Wave-maintained annual models of climate variability. *J. Clim.* **13**: 4414–4429.

Lin H, Derome J, Greatbatch RJ, Peterson KA, Lu J. 2002. Tropical links of the Arctic Oscillation. *Geophys. Res. Lett.* **29**: 1943, DOI: 10.1029/2002GL015822.

Lin H, Derome J, Brunet G. 2005. Correction of atmospheric dynamical seasonal forecasts using the leading ocean-forced spatial patterns. *Geophys. Res. Lett.* **32**: L14804, DOI: 10.1029/2005GL0 23060.

Liu ZY, Wu LX. 2004. Atmospheric response to North Pacific SST: the role of ocean-atmosphere coupling. *J. Clim.* **17**: 1859–1882.

Muller W, Appenzeller AC, Schar C. 2005. Probabilistic seasonal prediction of the winter North Atlantic Oscillation and its impact on near surface temperature. *Clim. Dyn.* **24**: 213–226.

Overland JE, Adams JM, Bond NA. 1999. Decadal variability of the Aleutian low and its relation to high-latitude circulation. *J. Clim.* **12**: 1542–1548.

Pacanowski RC, Griffies SM. 1998. *MOM 3.0 Manual*. NOAA/Geophysical Fluid Dynamics Laboratory, Princeton, NJ, 638.

Peng SL, Robinson WA, Li SL. 2003. Mechanisms for the NAO responses to the North Atlantic SST tripole. *J. Clim.* **16**: 1987–2004.

Qian ZL, Wang HJ, Sun JQ. 2011. The hindcast of winter and spring Arctic and Antarctic Oscillation with the coupled climate models. *Acta Meteorol. Sin.* **25**(3): 340–354.

Reynolds RW, Rayner NA, Smith TM, Stokes DC, Wang W. 2002. An improved in situ and satellite SST analysis. *J. Clim.* **15**: 1609–1625.

Rigor IG, Colony RL, Martin S. 2000. Variations in surface air temperature observations in the Arctic, 1979-1997. *J. Clim.* **13**(5): 896–914.

Semtner AJ. 1976. A model for the thermodynamic growth of sea ice in numerical investigations of climate. *J. Phys. Oceanogr.* **6**: 27–37.

Sun JQ, Ahn JB. 2011. A GCM-based forecasting model for the landfall of tropical cyclones in China. *Adv. Atmos. Sci.* **28**: 1049–1055.

Sun BM, Li CY. 1997. Relationship between disturbance of East Asian trough and tropical convection activities. *Chin. Sci. Bull.* **42**(5): 500–504 in Chinese.

Sun JQ, Wang HJ. 2006. Relationship between Arctic Oscillation and Pacific Decadal Oscillation on decadal timescale. *Chin. Sci. Bull.* **51**(1): 75–79.

Sun JQ, Wang HJ, Yuan W. 2008. Decadal variations of the relationship between the summer North Atlantic Oscillation and middle East Asian air temperature. *J. Geophys. Res.* **113**: D15107, DOI: 10.1029/2007JD009626.

Sun JQ, Wang HJ, Yuan W. 2009. Role of the tropical Atlantic sea surface temperature in the decadal change of the summer North Atlantic Oscillation. *J. Geophys. Res.* **114**: D20110, DOI: 10.1029/2009JD 012395.

Tang YM, Lin H, Derome J, Tippett MK. 2007. A predictability measure applied to seasonal predictions of the Arctic Oscillation. *J. Clim.* **20**: 4733–4750.

Thompson DWJ, Wallace JM. 1998. The Arctic Oscillation signature in the wintertime geopotential height and temperature fields. *Geophys. Res. Lett.* **25**: 1297–1300.

Thompson DWJ, Wallace JM. 2000. Annular modes in the extratropical circulation, part I: month-to-month variability. *J. Clim.* **13**: 1000–1016.

Thompson DWJ, Wallace JM. 2001. Regional climate impacts of the Northern Hemisphere annular mode. *Science* **293**: 85–89.

Thompson DWJ, Wallace JM, Hegerl GC. 2000. Annular modes in the extratropical circulation, part II: trends. *J. Clim.* **13**: 1018–1036.

Trilaksono NJ, Otsuka S, Yoden S. 2012. A time-lagged ensemble simulation on the modulation of precipitation over West Java in January-February 2007. *Mon. Weather Rev.* **140**: 601–616.

Wallace JM, Gutzler DS. 1981. Teleconnections in the geopotential height field during the Northern Hemisphere winter. *Mon. Weather Rev.* **109**: 784–812.

Wang J, Ikeda M. 2000. Arctic Oscillation and Arctic sea-ice oscillation. *Geophys. Res. Lett.* **27**: 1287–1290.

Wang HJ, Jiang DB. 2004. A new East Asian winter monsoon intensity index and atmospheric circulation comparison between strong and weak composite. *Quat. Sci.* **24**(1): 19–27 (in Chinese).

Wu B, Wang J. 2002. Winter Arctic Oscillation, Siberian High and East Asian winter monsoon. *Geophys. Res. Lett.* **29**(19): 1897, DOI: 10.1029/2002GL015373.

Yang S, Lau KM, Yoo SH, Kinter JL, Miyakoda K, Ho CH. 2004. Upstream subtropical signals preceding the Asian summer monsoon circulation. *J. Clim.* **17**: 4213–4229.

Yu RC, Zhou TJ. 2004. Impacts of winter-NAO on March cooling trends over subtropical Eurasia continent in the recent half century. *Geophys. Res. Lett.* **31**: L12204, DOI: 10.1029/2004GL019814.

Yuan W, Sun JQ. 2009. Enhancement of the summer North Atlantic Oscillation influence on Northern Hemisphere air temperature. *Adv. Atmos. Sci.* **26**(6): 1209–1214, DOI: 10.1007/s00376-009-8148-x.